10

Atomic Force Microscopy to Characterize the Healing Potential of Asphaltic Materials

Prabir Kumar Das, Denis Jelagin, Björn Birgisson and Niki Kringos
Railway and Highway Engineering, KTH Royal Institute of Technology
Sweden

1. Introduction

Worldwide, asphalt concrete is the most commonly used material for the top layer of pavements. The asphalt mixture's ability to provide the necessary stiffness and strength via its strong aggregate skeleton, while at the same time offering a damping and self-restoring ability via its visco-elastic bituminous binder, makes it a uniquely qualified material for increased driving comfort and flexible maintenance and repair actions. Unfortunately, bitumen supply is diminishing as crude sources are depleted and more asphalt refineries install cokers to convert heavy crude components into fuels. It is therefore becoming of imminent urgency to optimize the lifetime of the virgin bitumen from the remaining available crude sources. With 90% of the total European road network having an asphalt surface or incorporating recycled asphalt mixture in one of its base layers, the annual production of asphalt mixtures in Europe is well over 300 million tonnes. It is therefore fair to state that asphalt mixtures play a significant role in the economic viability and international position of the European pavement industry.

The intrinsic self-restoring ability of some bitumen, often referred to as its 'healing potential', could thereby serve as an excellent characteristic that could be capitalized upon. To date, however, there is still very little fundamental insight into what causes some bitumen to be better 'healers' than others. Even less is known about the resulting impact of this healing potential on the overall lifetime of the pavement. Healing potential is therefore very rarely included into pavement lifetime predictions or brought into the planning of maintenance operations, which is a missed opportunity. This will not change until a better understanding is created about the fundamental healing processes, which would allow for tailoring of bitumen during the manufacturing process and could potentially have a significant impact on an increased pavement service lifetime.

Current CE (European Conformity) specifications for bituminous binders do not contribute to advancing the understanding of the healing properties of the bitumen and even in more academic context; researchers often limit themselves to the performance of fatigue tests with and without rest periods from which an overall measure of the stiffness of the sample is calculated. The fatigued samples with rest periods may show a slower decrease of stiffness than the samples that were continuously fatigued. This ratio is then directly used as a quantification of the healing propensity of the bitumen during the rest periods. Yet it could be argued that part of this ratio can be contributed to the visco-elastic unloading behavior of

the material and says very little about the chemo-mechanical healing propensity, nor helps in understanding of the controlling parameters.

Bitumen is a complex mixture of molecules of different size and polarity, for which microstructural knowledge is still rather incomplete. As physical properties of bitumen are largely dependent on this microstructure, the prediction of the performance of asphalt pavements is also directly related to this. A detailed knowledge of microstructure is needed to understand the physico-chemistry of bitumen, which can serve as the direct link between the molecular structure and the rheological behaviour (Lesueur et al., 1996; Loeber et al., 1998). Optical microscopy techniques have been employed for more than three centuries to study the microstructure of materials (e.g. Baker, 1742). Researchers (Lu & Redelius 2005; Hesp et al., 2007) used optical microscopy in asphalt field to have a better understanding and visualization of bitumen microstructures. However, because of the opacity and adhesive properties of bitumen, optical microscopy has not received much attention from the asphalt industry. To overcome some of the limitations of optical microscopy, researcher in the asphalt field have chosen to use scanning probe microscopy such as the atomic force microscopy (AFM). AFM is capable of measuring topographic features at atomic and molecular resolutions as compared to the resolution limit of optical microscopy of about 200nm. Moreover, the AFM has the advantage of imaging almost any type of surface which opens the window for investigating microstructures of different polymers and wax modified bitumen.

2. Asphalt under the AFM – historic overview

In an effort to enhance the understanding and characterization of bitumen microstructure, atomic force microscopy (AFM) techniques have been employed to bituminous materials over the last 15 years. Typical image obtained from AFM scanning is depicted in Fig. 1, where one can easily observe the existing of microstructures in the bitumen matrix.

Loeber et al. (1996, 1998) was the first research group who published a inclusive investigation of bitumen using AFM. In these studies, bitumen samples were prepared by a heat-casting method to preserve the solid-state morphology. They revealed ripple microstructures with several micrometers in diameter and tens of nanometers in height. The authors named those rippled yellow and black strips microstructures ''bumble bees'' and attributed them to the asphaltenes (Redelius, 2009). Other shapes and textures including networks and spherical clusters were also observed in the study.

Based on Loeber's findings, Pauli et al. (2001) wanted to find the correlation between the ''bumble bee'' shaped microstructures and the amount of asphaltenes in the bitumen. In this study, they investigated solvent-cast films of bitumen under AFM using both friction-force and tapping mode. From these, they found the same Loeber's bee-shaped microstructures. To confirm that the bee-shaped structures were asphaltenes, they doped bitumen with asphaltenes and observed an increase in the density of bee-shaped microstructures. Their group also observed that the microstructure disappeared after repetitive scanning over the same area (Pauli & Grimes, 2003) and assumed the reason for this phenomenon was due to the red laser light of the AFM which produces heat and softening of the surface.

A research group from Vienna University of Technology (Jäger et al., 2004), investigated five different types of bitumen and also reported randomly distributed bee-shaped structures, which, just like the previous researchers they related to the asphaltenes in the bitumen.

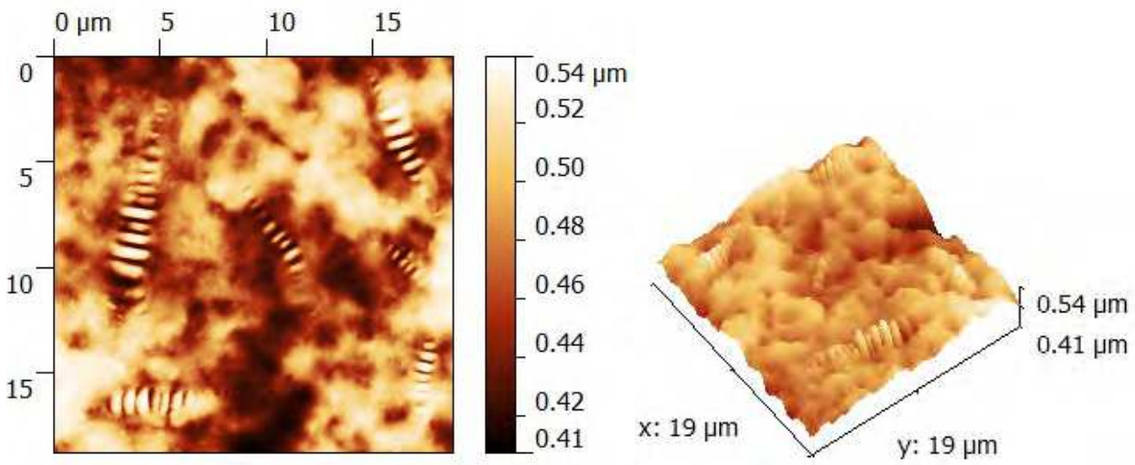

Fig. 1. Topographic 2D (left) and 3D (right) AFM image of bitumen indicating evidence of microstructures

Based on the obtained AFM images from non-contact mode and pulsed-force mode, four different material phases (i.e., hard-bee, soft-bee, hard-matrix and soft-matrix phase) were identified. However, they could not distinguish between soft-bee and soft-matrix phase as the relative stiffness for the two phases were more or less the same. After investigating the bee-shaped structures in the 5µm scale, the authors reported that the distance between the higher parts of the bees was approximately 550nm and appeared to be independent of the source of bitumen.

After this, Masson et al. (2006) conducted extensive AFM studies on the microstructure phases in bitumen by using 12 different types of Strategic Highway Research Program (SHRP) bitumen. In this study, bitumen samples were prepared by heat casting films onto glass plates. By using AFM phase detection microscopy (PDM), the detected four phases were defined as catanaphase (bee-shaped), periphase (around catanaphase), paraphrase (solvent regions) and salphase (high phase contrast spots), which were similar to those reported by Jäger et al. (2004). Interestingly, the researchers, for the first time, found very poor correlation between the asphaltene content and the bee-shaped structures. Furthermore, no correlation was found between the PDM results and the SARA fractions (S-satutares, A-aromatics, R-resins, A-asphaltenes) or acid-base contents of the observed bitumen. In addition, the area ratio of the catanaphase appeared to correlate with the mass parent of Vanadium and Nickel metals for several samples. The authors also reported different microstructures of the same bitumen samples prepared by heat casting and solvent casting. Continuing their study to bitumen stiffness at low temperatures under cryogenic AFM (Masson et al., 2007), at temperatures -10°C to -30°C, they showed that not all the bitumen phases contracted equally. The reason for this different contraction could be that the catana, peri and para phases were related to the existence of domains with different glass transition temperatures. One of the key findings of this low temperature AFM study was that bitumen with multiple phases at room temperature are never entirely rigid, even when well below the glass transition temperature.

De Moraes et al. (2009), studied the high temperature behaviour of bitumen using AFM at different temperatures followed by different rest periods. The authors observed that phase

contrast and topography images were highly dependent on storage time and temperature. This research group also observed the bee phase, a soft matrix phase surrounding the bee phase and a hard matrix dispersed on the soft phase, similar to findings reported by Jäger et al. (2004) and Masson et al. (2006). The authors also observed that the bee-shaped structure completely disappeared for samples at temperatures higher than 70°C and upon cooling to 66°C they began nucleating.

Concurrently, the changing microstructure after aging of bitumen was studied using AFM by Wu et al. (2009). In these studies, both neat and SBS polymer modified bitumen was aged using a pressure aging vessel (PAV). Comparing the obtained images before and after aging, the authors reported that the bee-shaped structure significantly increased after aging. To support the observed phenomena, the researchers related this to the production of asphaltene micelle structures during the aging process. These findings are consistent with the study by Zhang et al. (2011).

Tarefder et al. (2010a, 2010b) studied nanoscale characterization of asphalt materials for moisture damage and the effect of polymer modification on adhesion force using AFM. They observed wet samples always showed higher adhesive force compared with dry one. The authors concluded that the adhesion behaviour of bitumen can vary with the chemistry of the tip and functional groups on it.

Recently, Pauli et al. (2009, 2011) reported that all of these interpretations, including their previous findings were at least partially wrong and came up with a new hypothesis in which they stated that the ''bees are mainly wax". To prove their hypothesis, they scanned different fractions of bitumen and found bee-shaped structures even in the maltenes which contain no asphaltenes, while the de-waxed bitumen fractions did not show any microstructures. The authors concluded that the interaction between the crystallizing paraffin waxes and the remaining bitumen are responsible for much of the microstructuring, including the well-known bee-shaped structures. They also reported sample variables such as film thickness, the solvent spin cast form, and the fact that solution concentration could also strongly influence the corresponding AFM images.

Even though different research groups concluded significantly different reasons for the structures to appear, the extensive atomic force microscopy (AFM) studies showed that bitumen has the tendency to phase separate under certain kinetic conditions and is highly dependent on its temperature history. Besides focusing on the reasons behind the microstructure growth, it is also important to relate these microstructures to the performance of bitumen.

3. Utilizing the AFM images as a basis for asphalt healing model

From Atomic Force Microscopy (AFM) scans, it was found that bitumen is not a homogeneous bulk material as microstructures are observed in almost all the bitumen (Loeber et al., 1996, 1998; Pauli et al., 2001, 2009, 2011; Jäger et al., 2004; Masson et al., 2006). All the previous studies showed that bitumen appeared to have some form of 'phase separation' dependence on its temperature history, storage time and crude source. Changing the temperature of the bitumen showed a movement of the phases and sometimes resulted in an overall homogeneous material, where the clusters seem to have 'melted' back into the matrix structure. The ability of bitumen to phase separate and redistribute its phases

depends on the thermal or mechanical energy input. Recently, based on this phase separation phenomena under certain kinetic conditions, Kringos et al. (2009a) developed a healing model by assuming the bitumen matrix has two types of phases (i.e., phase α and phase β), as shown in Fig. 2.

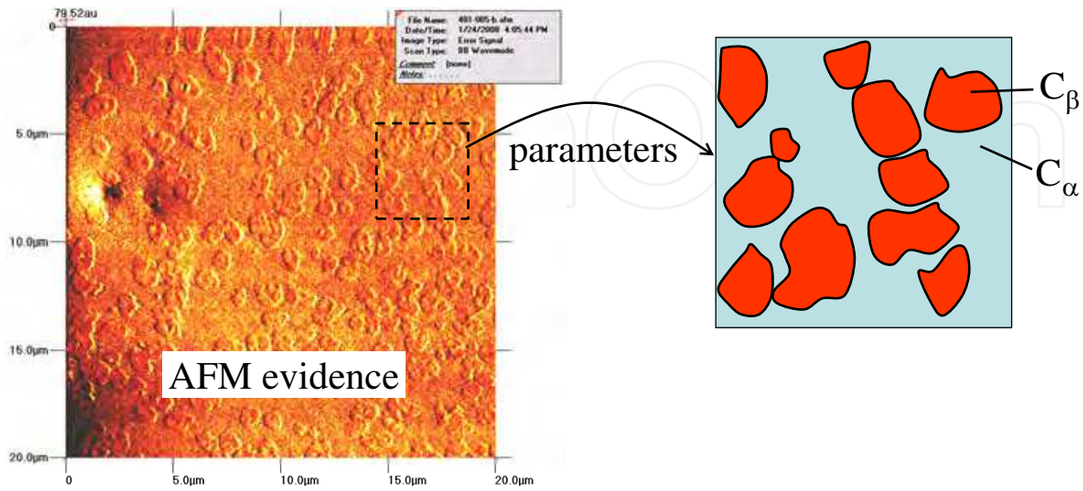

Fig. 2. AFM evidence of phase separation in bitumen (Pauli et al., 2011)

3.1 Postulated healing mechanism

From mechanical considerations, it is known that the interfaces between two materials with different stiffness properties serve as natural stress inducers. This means that when the material is exposed to mechanical and or environmental loading, these interfaces will attract high stresses and are prone to cracking. On this scale, this would result in a crazing pattern, which can be detected on a higher (macro) scale by a degradation of the mechanical properties of the material, such as the stiffness or fracture strength. If this process would continue, these micro-cracks (or crazes) would continue developing, start merging and finally form visible cracks.

A finite element simulation done by Kringos et al. (2012) demonstrated the concept of diminished response and the introduction of high stresses in an inhomogeneous material, as shown in Fig. 3, for a constant displacement imposed on a homogeneous and an inhomogeneous bitumen. The bituminous matrix is hereby simulated as a visco-elastic material and the inclusions as stiff elastic. From the deformation pattern it can be seen that the inhomogeneous material acts not only stiffer, but is no longer deforming in a smooth, uniform, manner and high stresses appear from the corners of the stiffer particles.

From the bitumen AFM scans it was shown that many bitumen sapmles, under certain circumstances, will form such inhomogeneities. If then, by changing the thermodynamic conditions of the material by inputting thermal or mechanical energy, these inclusions rearrange themselves or disappear; restoration of the mechanical properties would appear on a macro-scale. Since the phase-separation is occurring on the nano-to-micro scale, the interfaces between the clusters and the matrix could start crazing when exposed to (thermo) mechanical loading. A change of these clusters, either by rearranging themselves or by merging into the main matrix, would then lead to a memory loss of these micro-crazes and

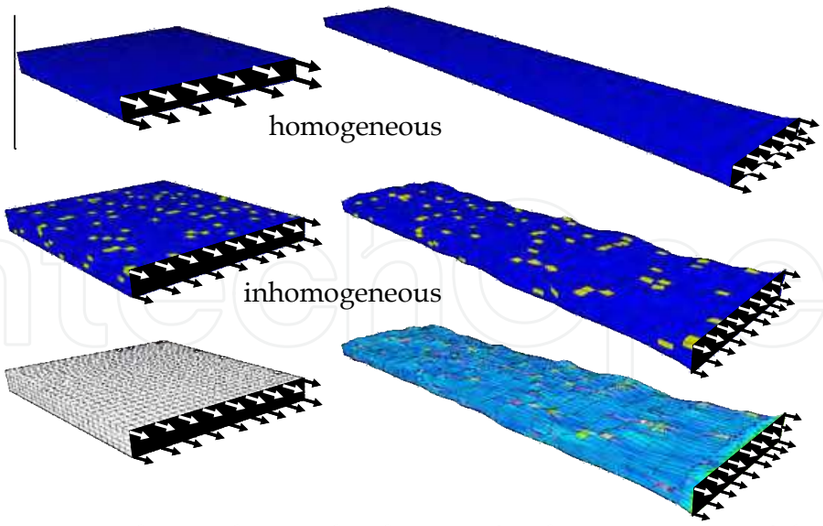

Fig. 3. Displacement and normal stress development in a homogeneous vs. inhomogeneous bitumen (Kringos et al., 2012)

the bitumen would show a restoration of its original properties, which may be referred to as physico-chemical "healing". The driving force for the rearrangement of the phases upon a changed thermodynamic state is explained in the following section.

3.2 Governing equations

To develop the governing equations for the phase-separation model, the general mass balance equation can be expressed as

$$\rho \frac{\partial_\alpha c}{\partial t} - \mathrm{div}\left(\rho_\alpha \underset{\sim}{M} \cdot \nabla_\alpha \mu\right) = 0 \tag{1}$$

where $_\alpha\rho = \frac{_\alpha m}{V}$ is the density, $_\alpha\mu$ is the chemical potential and $_\alpha\underset{\sim}{M}$ is the diffusional mobility tensor of phase α in the material.

The chemical potential μ_α can be written as the functional derivative of the free energy Ψ :

$$_\alpha\mu = \frac{\delta\Psi}{\delta_\alpha c} \tag{2}$$

The free energy is composed of three terms

$$\Psi = \Psi_0 + \Psi_\gamma + \Psi_\varepsilon \tag{3}$$

where Ψ_0 is the configurational free energy, Ψ_γ is the Cahn Hilliard surface free energy and Ψ_ε is the strain energy.

Solving these equations, allows for the simulation of phase separation from various starting configurations. The free energy potentials and the mobility coefficient are hereby the

important input parameters to the model and need to be determined for the individual bitumen samples. In Fig. 4 a comparison between AFM scans and the model is given for three different bitumen samples. More details about the analyses can be found in Kringos et.al. (2012).

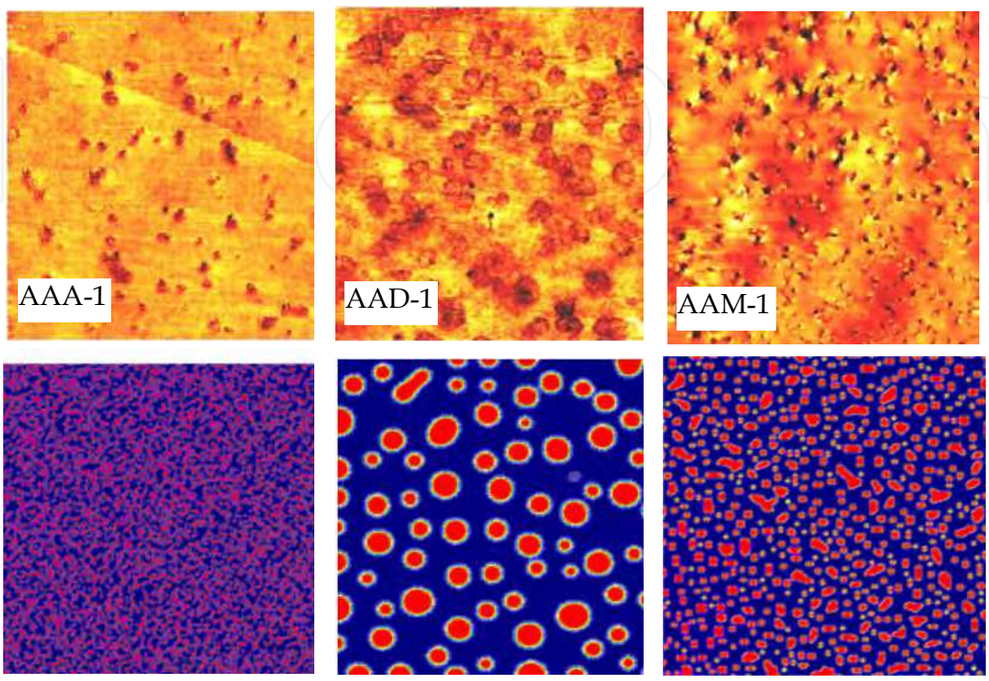

Fig. 4. Comparison between AFM scans and computed phase configuration (Kringos et al., 2012)

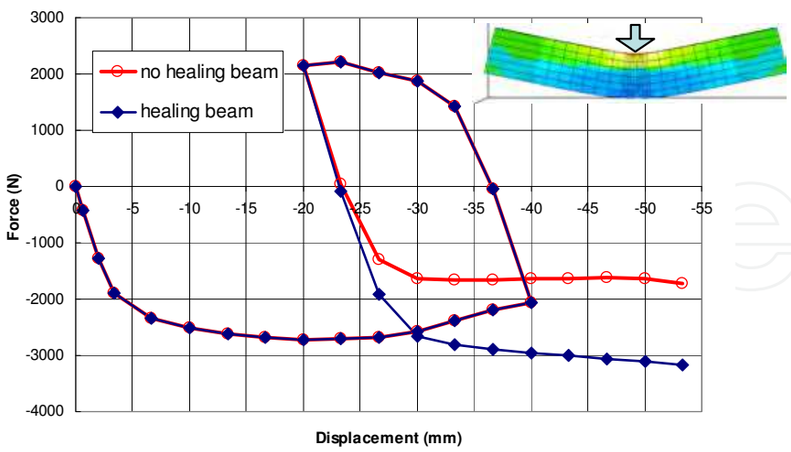

Fig. 5. Simulation of healing versus no-healing asphalt beam (Kringos et al., 2012)

The model can also be utilized in an 'upscaled' manner, in which the rearrangement of the phases, the appearance and thickness of the interfaces are linked to a healing function that becomes an intrinsic parameter that controls the evolution of dissipated energy. More details on the equations of this model and the parameters can be found from Kringos et.al.

(2009b). The force versus displacement diagram is shown for a simulation of a fatigue test using this model. It can be seen from the graphs that in the case on the 'healing beam' the material has lost its memory of the previous loading cycle, whereas in the case of the 'no-healing beam' the material is considerably weaker after the first loading cycle.

4. Healing model parameters

A parametric analysis performed by Kringos et al. (2012) investigated the effect of the various model parameters on the resulting phase configuration. In the simulations a mesh of 50 μm x 50 μm is simulated, similar to the size of the bitumen scans under the AFM. The time and space increments are normalized with respect to each other.

The initial t_0 configuration is represented by a homogenous mixture with a random perturbation, also known as a spinodal composition. Depending on the chosen parameters, different phase separation patterns will form. In the following, the influence of these parameters is shown by varying their values.

For the Cahn Hilliard parameter of $\kappa_2 = 0.0005$ and an average start concentration of 0.5 with random fluctuations of zero mean and no fluctuation greater than 0.01, results in the configurations at different time steps shown in Fig.6.

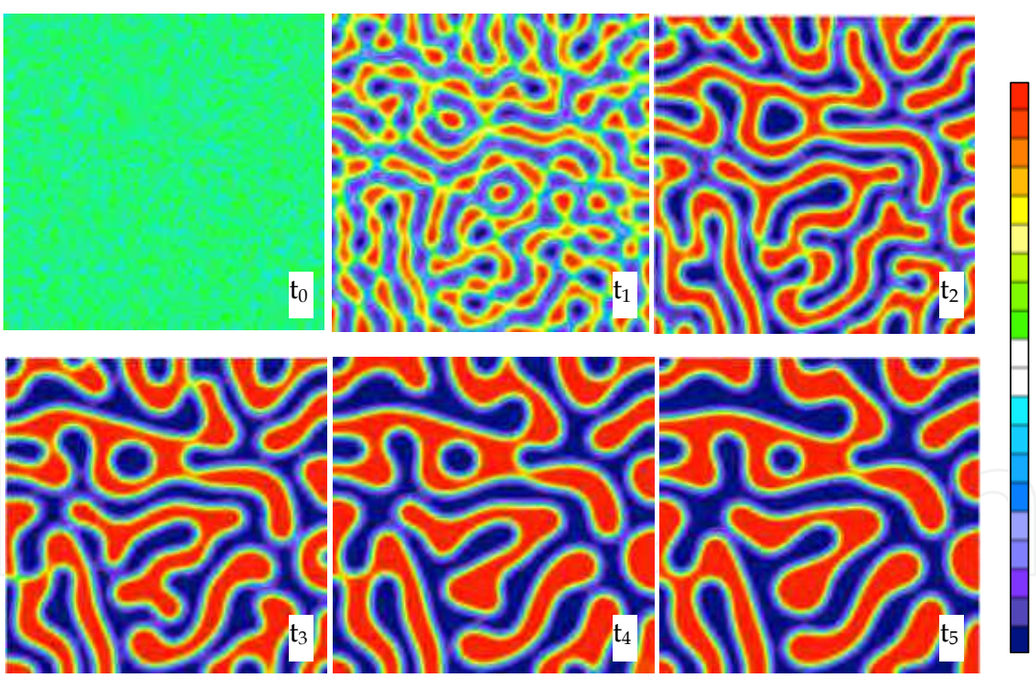

Fig. 6. Spinodal composition resulting in polymer-like phase separation (Kringos et al., 2012)

Keeping the parameters constant, but now changing the initial configuration to a maximum fluctuation of 0.05 results in a different end configuration as is shown in Fig. 7, which resembles better the phase configuration of bitumen as is seen under the AFM scans.

The Cahn Hilliard parameters are often expressed as ε which is related to the κ_2 via $\varepsilon^2 = \kappa_2$. The effect of this parameter is shown in Fig. 8.

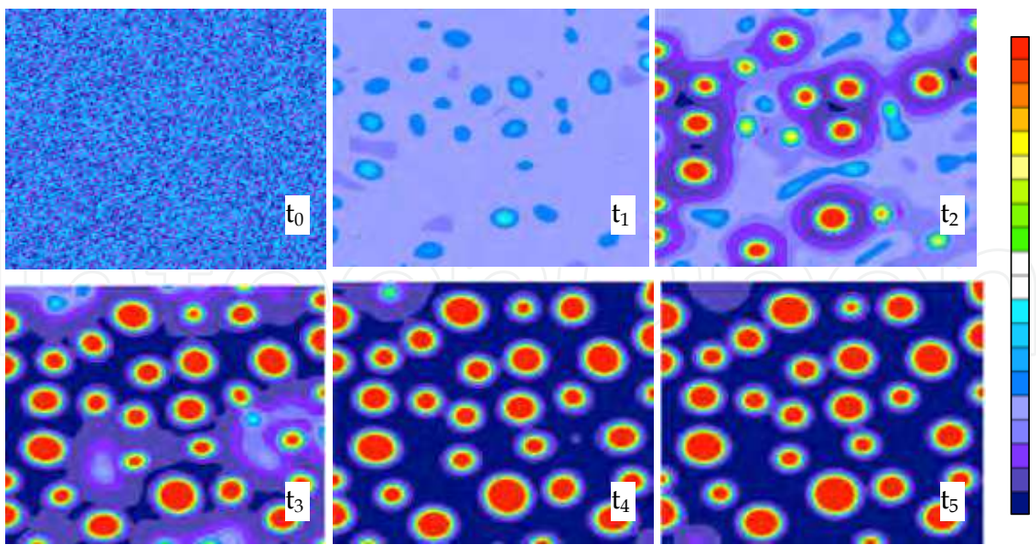

Fig. 7. Spinodal composition resulting in bee structure formation (Kringos et al., 2012)

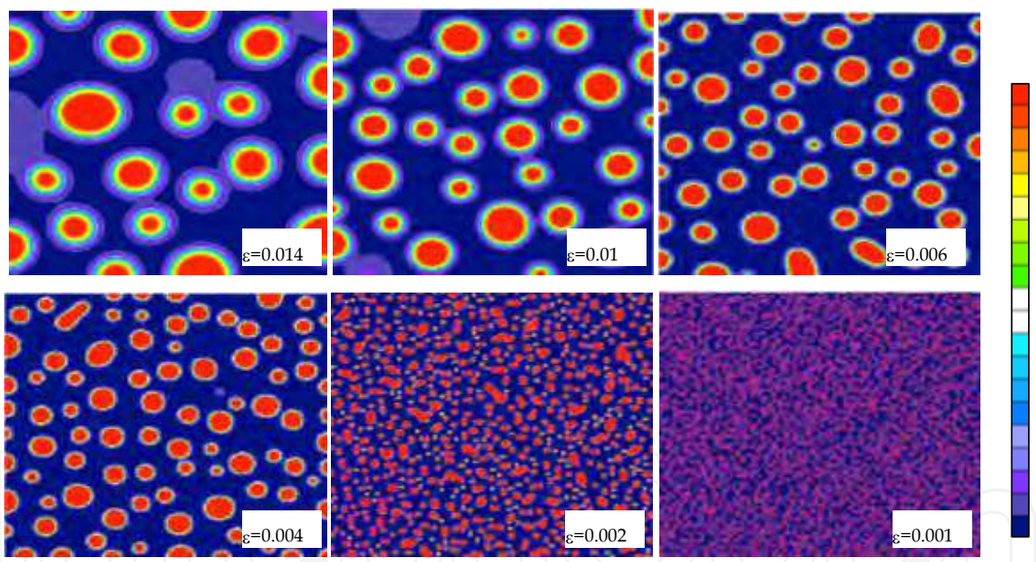

Fig. 8. End configurations with varying Cahn Hilliard parameter (Kringos et al., 2012)

Defining the matrix, the distinct phases (the bees) and the interfaces (IF) as the three fractions in the end configuration, the normalized fractions are plotted as a function of the varying Cahn Hilliard parameter, Fig. 9. As can be seen from the graph, an increased Cahn Hilliard parameter causes an increased interface (IF) fraction. Since this parameter controls the gradient energy distribution this result seems certainly logical. Interestingly thought, it can also be seen that both the matrix and the bees seem reduced. Which means that with an increased gradient distribution coefficient fewer bees are formed with thicker interfaces.

Changing the configurational free energy function whereby normalizing the energy barrier as shown in Fig. 10 (a) has the effect shown in Fig. 10 (b).

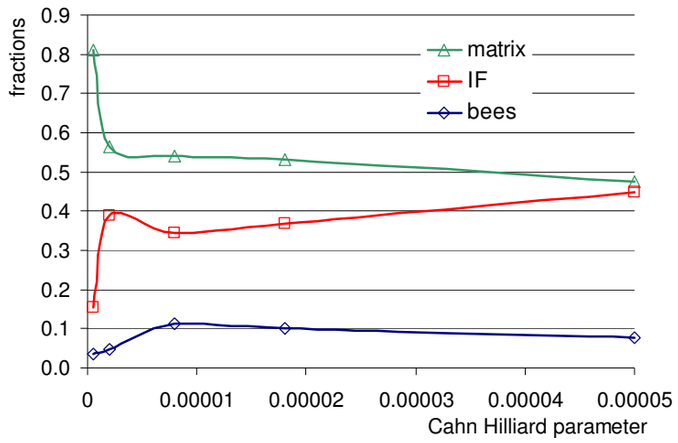

Fig. 9. Relationship between fractions and Cahn Hilliard parameter (Kringos et al., 2012)

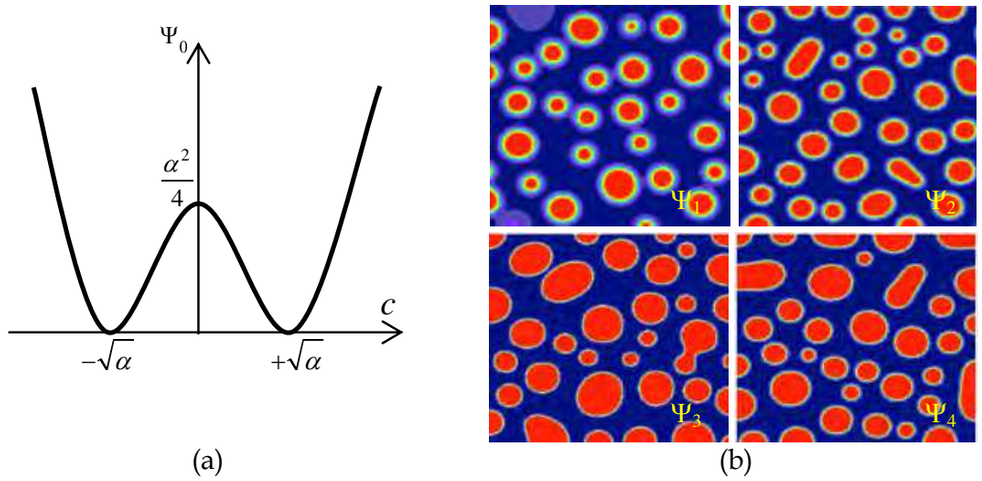

(a) (b)

Fig. 10. (a) Normalized .. potential (b) Changing Ψ_0; α =1, 2, 4 and 6 for $\Psi_1 - \Psi_4$ (Kringos et al., 2012)

5. Mechanical properties of the phases

As was discussed in the previous sections, it is important to know the properties of the bitumen phases with respect to its surrounding matrix, which is also needed for the healing simulation in the next section, Fig. 11. The rheology at various temperatures of the individual phases turned out to be more challenging than anticipated, so to get the parameters needed for the individual phases for the healing simulation, in this section a finite element analyses is performed. In this analysis the overall bitumen properties as determined in the previous section is used.

For each case the equivalent stiffness ratio is calculated from E_{case}/E_{caseA}

where case A represents an homogeneous mesh without any phase separation. The subscript m refers to the matrix properties and the subscript b refers to the bee structures. Using the phase separated configuration as shown in Fig. 12, the properties of the matrix were varied in the analyses while assuming the bee properties remained constant at $E_b = 2E_0$ and $\eta_b = 10\eta_0$.

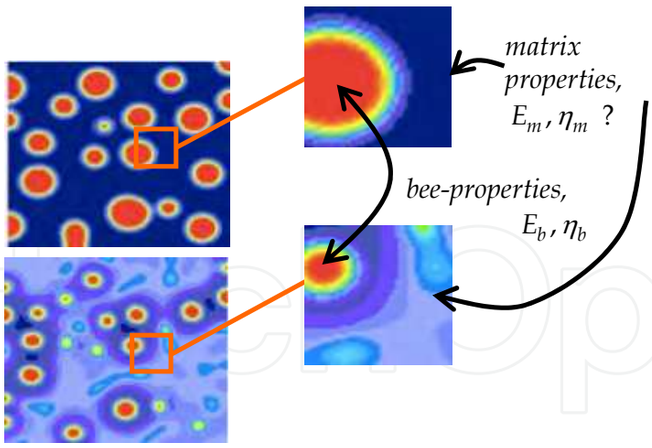

Fig. 11. Properties of bees and surrounding matrix (Kringos et al., 2012)

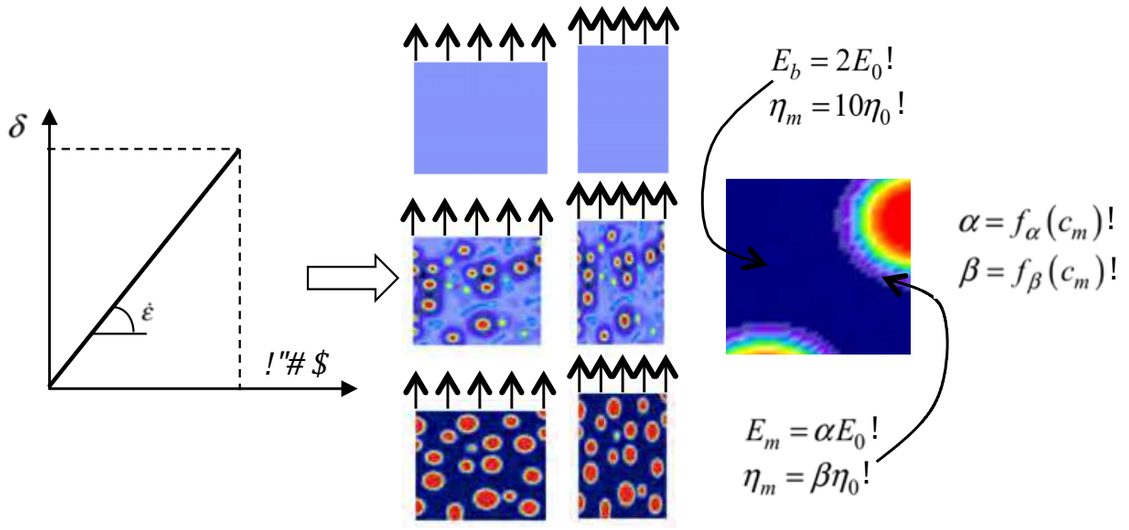

Fig. 12. Simulation of constant displacement test (Kringos et al., 2012)

From Table 1 the chosen matrix properties and the calculated equivalent stiffness at time 0.08 s is shown. In Fig. 13 the equivalent stiffness over the entire direct tension test is plotted.

Case	Configuration	E_m	η_m	Equi.stiffness ratio @ t=0.08s
A	Homogeneous	E_0	η_0	1.00
B	Phase separated	E_0	η_0	1.06
C	Phase separated	$0.5E_0$	$0.1\eta_0$	0.56
D	Phase separated	$0.5E_0$	η_0	0.82
E	Phase separated	$0.9E_0$	η_0	1.02
F	Phase separated	$0.85E_0$	η_0	1.00

Table 1. Determined parameters

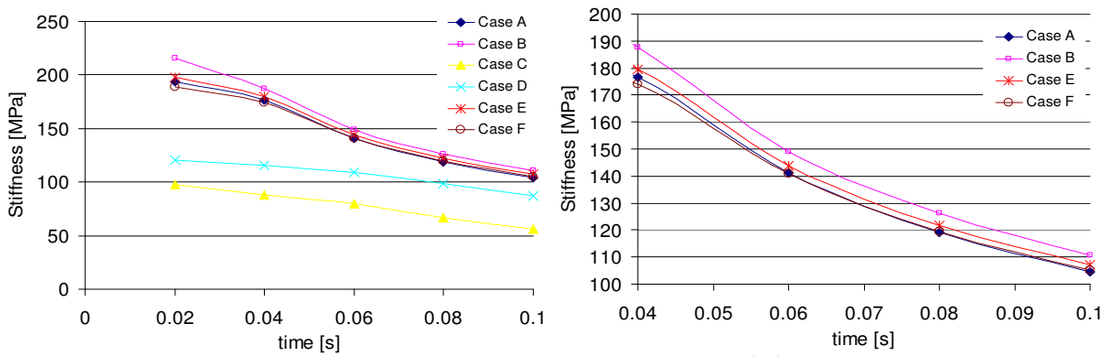

Fig. 13. Calculation of equivalent stiffness for direct tension cases (Kringos et al., 2012)

In the case of the homogeneous configuration, the overall matrix normalized concentration is 0.5 , in the case of the phase separated configuration, the minimum normalized concentration of the bees is -1 and the maximum normalized concentration of the matrix is +1, Fig. 14. Based on this, the following relationship is formed:

$$E_m = \alpha E_0 \quad ; \quad \alpha = (0.84+0.34C) - 1$$

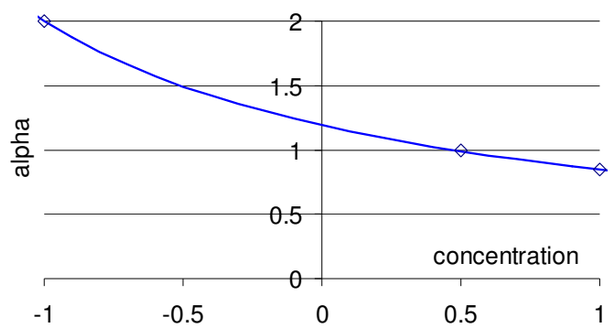

Fig. 14. Alpha as a function of normalized concentration (Kringos et al., 2012)

6. Simulation of healing in bitumen

Using the parameters as described in the previous sections, in this section the developed healing model will be demonstrated. For this, three different cases have been selected, Fig. 15.

In all cases a mesh of 50 μm x 50 μm was exposed to six displacement controlled tension and compression loading cycles. In case A, this was done continuously without any rest periods between the cycles. In case B and C, a rest period was applied after the first three loading cycles. For case B, during this rest period the material was allowed to visco-elastically unload. In case C, in addition to the visco-elastic unloading, the material was allowed to rearrange its phases, based on the PS model as was shown in the earlier sections. The initial material configuration in all simulation was the phase-separated configuration as was computed in Fig. 7. In the simulation, the mechanical properties for the matrix and the bees as derived earlier in this chapter and the energy based elasto-visco-plastic constitutive model briefly described earlier were utilized.

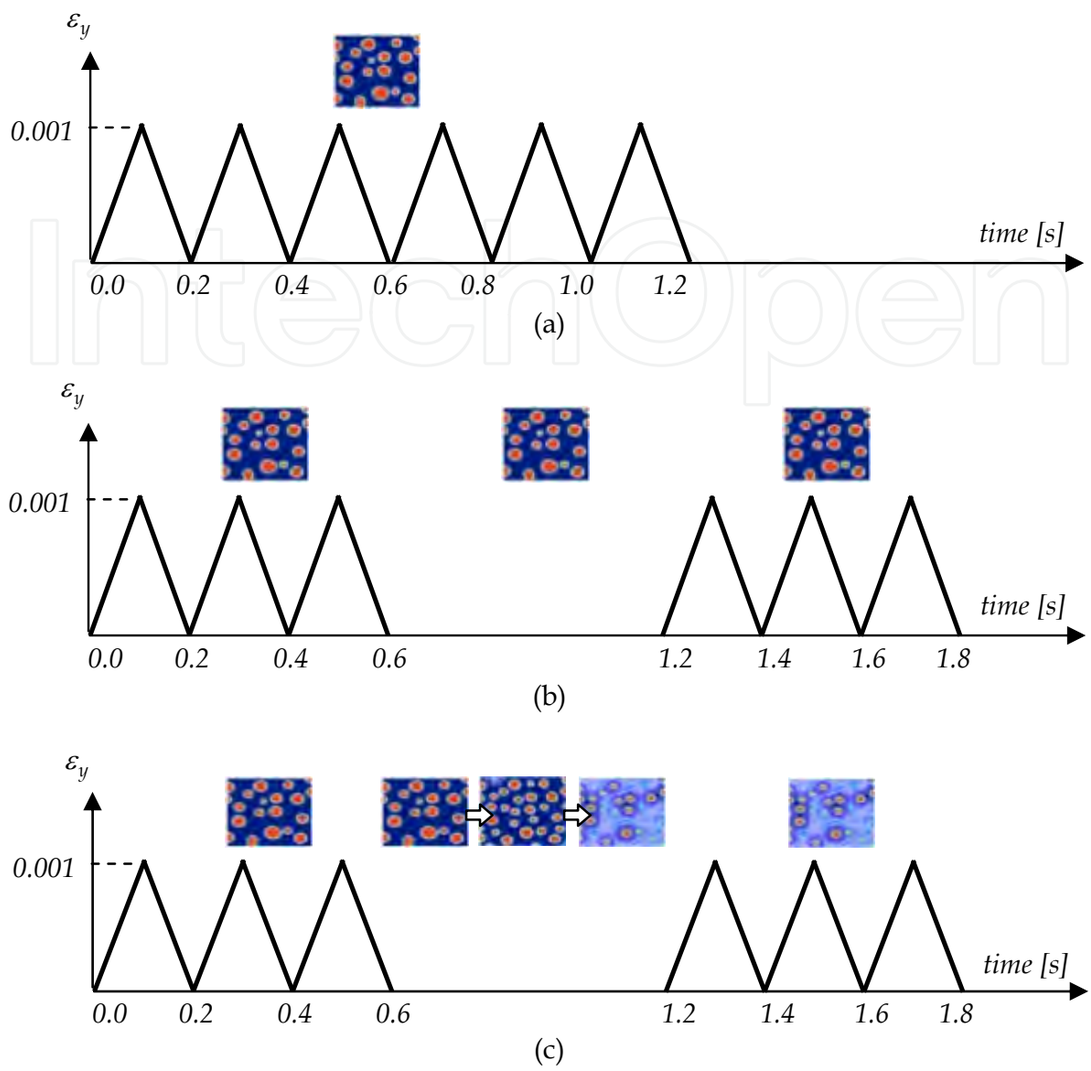

Fig. 15. Fatigue simulation (a) with no rest period (b) with VE unloading during rest period (c) with phase rearrangement during rest period (Kringos et al., 2012)

In Fig. 16 and Fig. 17 the evolution of the normal stress and damage development are shown for the simulated time steps, respectively. Damage is hereby defined as equivalent plastic strain, or permanent deformation.

What is very noticeable from the stress and damage development plots is the inhomogeneous development of the stresses and damage throughout the material. Additional it can be noticed from the damage graphs that the damage originates from the interface areas between the bee structures and the matrix.

In Fig. 17 the damage development at a chosen location in the simulated mesh is plotted as a function of the loading cycles and loading time. From these graphs it can be seen that case B has generated less damage than case A after the six loading cycles. By comparing with case C, that also included the phase rearrangement based on the kinetics of the material, it can be seen that even less damage was generated in comparison with case A and B.

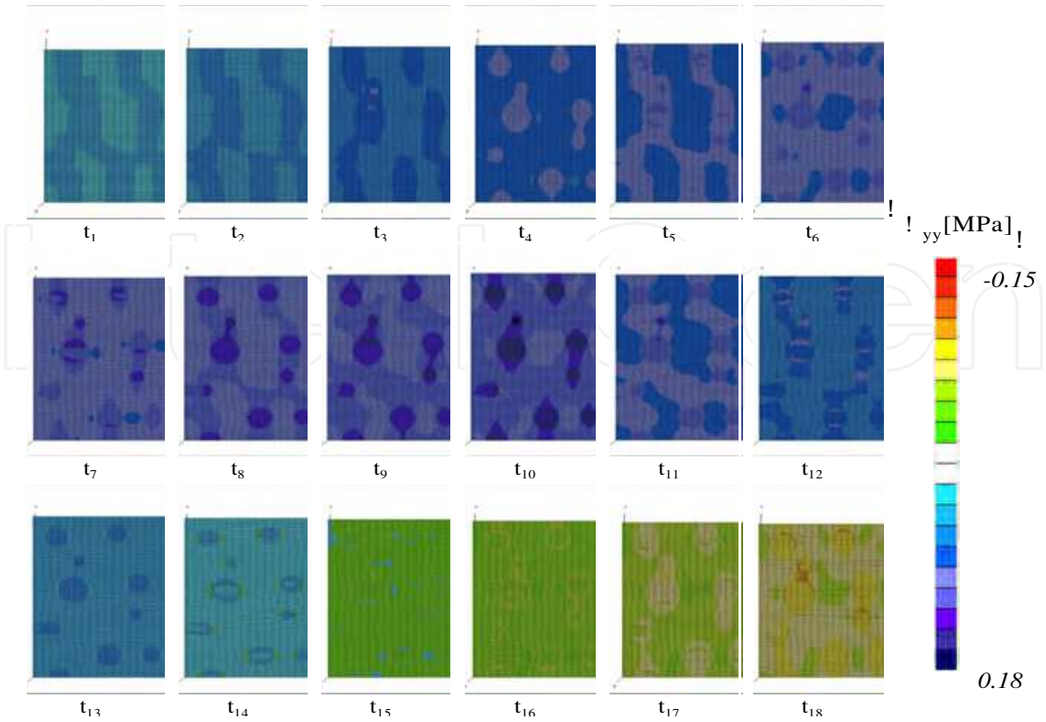

Fig. 16. Stress development during fatigue simulation (Kringos et al., 2012)

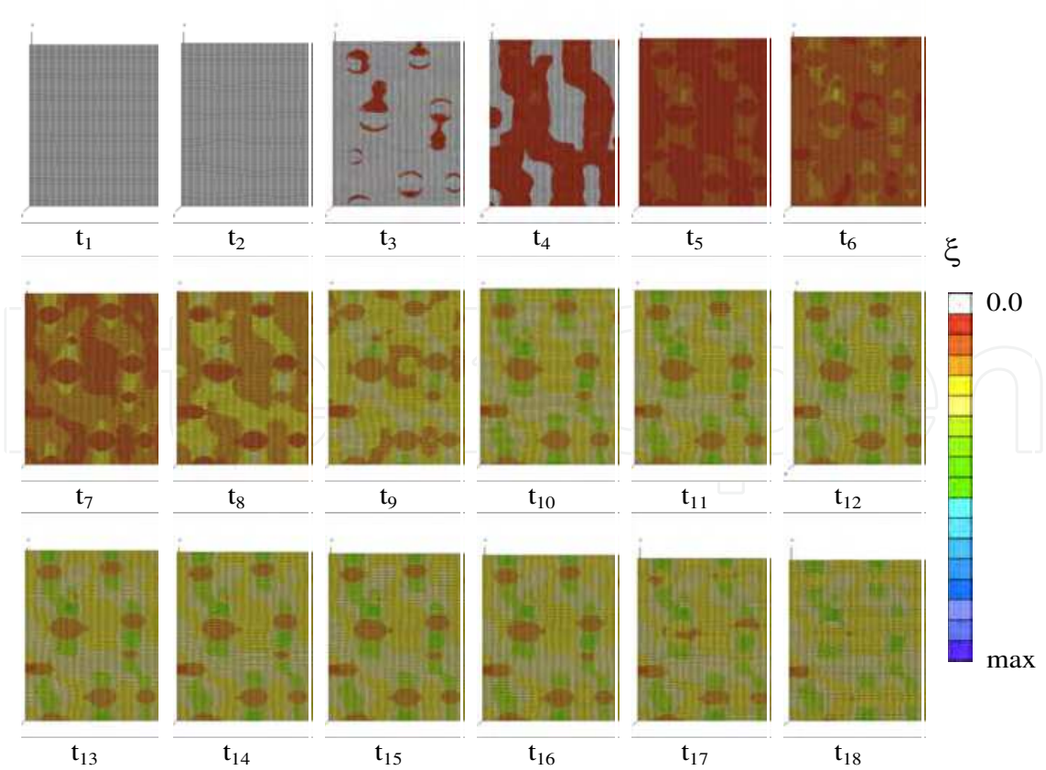

Fig. 17. Damage ξ development during fatigue simulation (Kringos et al., 2012)

Keeping in mind that these plots are made for a given location in the material, the equivalent stiffness of the overall mesh was also determined, Fig. 18. From these graphs it can be seen that case B again showed a lesser reduction of the intial stiffness after the six loading cycles as compared with case A. Case C showed even more restoration of the equivalent stiffness in comparison with case A and B.

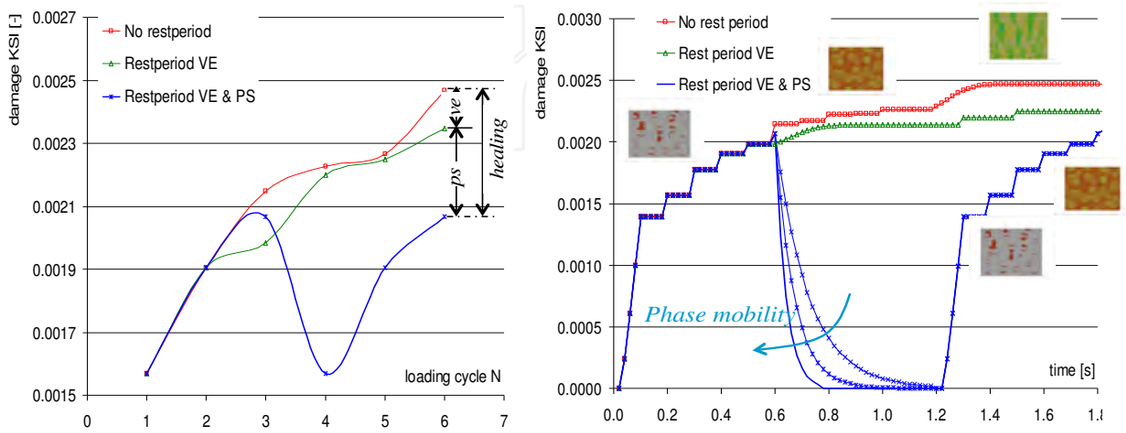

(a) (b)

Fig. 18. Simulation of damage and healing development (Kringos et al., 2012)

From these analyses is can be concluded that the 'healing' propensity of bitumen which is generally quantified by a fatigue test, could be partly due to visco-elastic loading and partly due to the healing mechanism that was presented in this chapter. If this is indeed the case, this would have important implications for the in time development of the healing propensity of asphalt pavements in the field.

Moreover, the two contributions (visco-elasticity and phase rearrangements) are controlled by completely different parameters. Which is important to understand when one wants to optimize the healing potential of an asphaltic mixture.

For instance it can be seen from Fig. 18 (b) that by varying the phase mobility, the rate of healing can be changed. This would mean that the applied rest periods in laboratory healing tests or the breaks between traffic loading on asphalt pavements would have important effects on the healing of generated damage. It is very well possible that some bitumen have intrinsic healing capacity, but due to a relatively low mobility of the phases, this is never maximized in practice. This would mean that if bitumen producers could change something in the bitumen blend to increase the mobility of certain phases, the healing propensity could be optimized.

The material properties of the individual phases are of paramount importance for the mechanical properties and the healing capacity of the entire bitumen. In the previous section the phase scans of bitumen under the AFM were discussed. The AFM can also be utilized to determine the material properties as well as the scanned phases simultaneously. The difficulty with observing bitumen using AFM is its viscoelastic nature and its highly temperature dependent flow behavior. In the following section, the utilization of AFM to determine material properties of bituminous phases is discussed in more details.

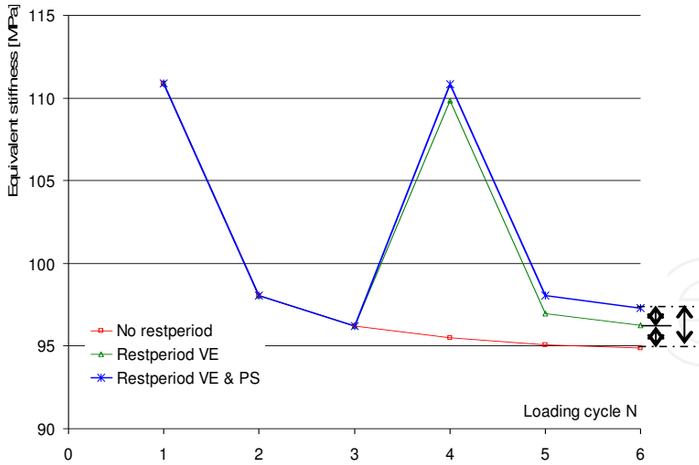

Fig. 19. Calculation of equivalent stiffness (Kringos et al., 2012)

7. Nano-indentation

Instrumented indentation testing, a test method where load and depth of indentation are continuously monitored, have become a common technique for characterizing mechanical behavior of a large variety of materials. Indentation testing is one of the few experimental techniques that can be performed at both large and small scales, thus allowing for the investigation of materials behavior across length scales from milli- to nanometers. The stress field induced by indenter in the specimen is highly localized, and the scale is proportional to the contact area. Thus by varying the indenter geometry, and size, as well as the applied load, one may obtain results representative for the material behavior on different scales. By using high-resolution testing equipment, the material properties can be measured at the micro- and nanometer level, thus allowing for a study of the variability in material properties across a specimen (Oliver & Pharr, 1992, 2003). Over the past 20 years, this technique has been used to investigate the linear elastic, viscoelastic and plastic properties of thin films, modified surfaces, individual phases in alloys and composites and other microscopic features. A detailed account of work done in this field has recently been given by (Gouldstone et al., 2007).

Recently number of attempts have been reported in the literature to use AFM in force mode to obtain elastic and viscoelastic properties of different materials, cf. e.g. (Tripathy & Berger, 2009; Gunter, 2009). AFM allows measurement of viscoelastic material properties with spatial resolution on the nanoscale; furthermore by performing the repetitive measurements at different temperatures or before and after oxidation it allows for the observance of different phases of the material. These data can be a key to understanding the governing mechanisms behind healing and ageing phenomena in bituminous binders.

The heart of any indentation testing is a method to extract the material parameters from the experimentally observed relation between indentation force F , and indentation depth, h . Modelling the indentation of viscoelastic solids thus forms the basis for analyzing the indentation experiments. Lee & Radok made substantial progress, by solving the problem of sphere indenting linear viscoelastic halfspace (Lee & Radok, 1960). Analogous results for the case of conical indenters were presented by (Graham, 1965), and for a flat punch by (Larsson & Carlsson, 1998). Huang & Lu (2007) developed a semi-empirical solution for viscoelastic

indentation of the Berkovich indenter. In AFM, a probe consisting of a cone with a nominal tip radius on the order of 10 nm or higher is typically used. The accurate determination of the AFM tip shape is in fact one of the major sources of uncertainty, when performing nanoindentation testing with AFM, particularly at lower load levels. As it has been argued by many investigators, in indentation testing at micro- and nanoscales it is very difficult to make a valid assumption concerning the indenter geometry, cf. e.g. Korsunsky (2001) and Giannakopoulos (2006). Even the best attempts at preparing a perfectly round spherical or perfectly sharp conical shapes inevitably produce flattened imperfect shapes. These deviations of the indenter shapes from the assumed ideal shape will affect measurements performed at small scales. The AFM tip is normally considered to be of conical shape with round spherical tip. The contact geometry is thus dominantly controlled by the spherical indenter tip at low load levels and is switching to conical geometry at higher loads. The procedure to extract viscoelastic properties with spherical indentation is illustrated below (Larsson & Carlsson, 1998)

Using ordinary notation the stress-strain relations for linear viscoelastic solids can be formulated in relaxation form as:

$$s_{ij}(t) = \int_0^t G_1(t-\tau)\frac{d}{d\tau}e_{ij}(\tau)\,d\tau \tag{4a}$$

$$\sigma_{ii}(t) = 3\int_0^t G_2(t-\tau)\frac{d}{d\tau}\varepsilon_{ii}(\tau)\,d\tau \tag{4b}$$

where

$$s_{ij} = \sigma_{ij} - \frac{1}{3}\delta_{ij}\sigma_{kk}, \qquad e_{ij} = \varepsilon_{ij} - \frac{1}{3}\delta_{ij}\varepsilon_{kk} \tag{5}$$

are the deviatoric components of stress and strain. In equations (4a) and (4b), G_1 and G_2 are the so-called relaxation functions in shear and dilation, respectively. The viscoelastic Poisson's ratio, $\nu(t)$, is related to the relaxation functions in equations (4a) and (4b) as:

$$\overline{\nu(s)} = \frac{1}{s}\frac{\left(\overline{G_2(s)} - \overline{G_1(s)}\right)}{\left(2\overline{G_2(s)} - \overline{G_1(s)}\right)} \tag{6}$$

using Laplace transformed quantities according to

$$\overline{f}(s) = \int_0^\infty f(t)e^{-st}\,dt \tag{7}$$

In principle, in order to completely characterize the viscoelastic material one needs to determine two independent viscoelastic functions $G_1(t)$ and $G_2(t)$. However, these two functions cannot be determined uniquely from experimental force-displacement data. Thus in most conventional testing techniques a constant viscoelastic Poisson's ratio is assumed,

and nanoindentation measures only the relaxation compliance in shear, cf. e.g. Giannakopoulos (2006) and Jäger et al. (2007). The shear relaxation function G_1 is expressed then as Prony series and the introduced constants are then determined in order to best fit the experimental results.

The relaxation test with AFM is performed by programming the tip to indent the specimen to a specified depth, $h(t)$, and then to hold the penetration depth constant for a specified time, i.e. $h(t) = h_0 H(t)$, $H(t)$ being the Heaviside function. Provided that the indenter is stiff as compared to the sample, the relation between G_1 and the indenter load measured as a function of time, $P(t)$, is given than as:

$$G_1(t) = \frac{6R(1-\nu)P(t)}{8a_0^3} \tag{8}$$

where R is the radius of curvature of the spherical indenter tip and a_0 is the maximum radius of the contact area defined as:

$$a_0^2 = (Dh_0)/2 \tag{9}$$

Equation (8) may be used to obtain shear relaxation modulus, provided that constant Poisson's ration is known, the material response is linear and the contact geometry is spherical. Equation (9) provides a simple way to check the linearity of the material response. As it has been show by Larsson & Carlsson (1998), the size of the residual impression in the specimens surface is very close to the maximum size of the contact area. One may thus follow AFM indentation testing with AFM scanning in tapping mode to measure size of the residual impression and compare it with the maximum contact radius predicted by equation (9). The discrepancy between the measured and predicted contact radii would indicate the presence of non-linear material effects. The assumption of the constant Poisson's ratio may not be satisfactory for characterization of bituminous binders, as volumetric material response may also exhibit spatial variation. Researchers have been attempting to address this issue and distinguish dilation and shear compliances by using secondary sensors to measure circumferential strain at a small distance from the contact area, e.g. Larsson & Carlsson (1998) or by comparing force-displacement relations for indenters with different shapes, e.g. Huang & Lu (2007). In particular, Larsson & Carlsson (1998) derived the following relations between $G_1(t)$, $G_2(t)$ and $P(t), \varepsilon_\theta$:

$$\int_0^t G_1(\tau)\,d\tau = \frac{6R}{8a_0^3}\int_0^t P(t-\tau)\big(1-\nu(\tau)\big)\,d\tau \tag{10}$$

$$\int_0^t \varepsilon_\theta(r, t-\tau)\big(1-\nu(\tau)\big)\,d\tau = -\frac{4a_0^3}{6\pi R r^2}\int_0^t \big(1-2\nu(\tau)\big)\,d\tau \tag{11}$$

Equations (10) and (11) are uncoupled Fredholm integral equations of first and second kind respectively. The technique required to solve such a system of equations numerically is well documented, cf. e.g. Andersson & Nilsson (1995).

Huang & Lu (2007) suggested to use the semi-empirical force-displacement relations for the Berkovich indenter along with the analytical solution for the spherical indenters as two independent equations for establishing $G_1(t)$ and $G_2(t)$. The relaxation functions may be then expressed as Prony series and their coefficients may be found as the best fit of the experimental data.

It has to be pointed out however that both of these approaches appear to be questionable when applied to AFM indentation testing: instrumenting the specimens surface with additional sensors appears not to be practically feasible at the length scale in question; at the same time the approach presented in Huang & Lu (2007) would require AFM tips with two distinct well defined shapes. Furthermore, the possibility to accurately measure linear viscoelastic material behavior with sharp indenters, such as Berkovich or conical, has been questioned by several researches, cf. e.g. Vanlandingham et al. (2005). The reason is that sharp indenters inevitably introduce intense strains local to the indenter tip, thus making the assumption of linearity invalid.

It may be concluded from the above that using AFM in force mode provides a useful tool to obtain at least qualitative information regarding the bitumen properties at nano-scale and their evolution with temperature and oxidation. The use of AFM to obtain absolute quantitative estimates of viscoelastic properties of the bituminous binders appears however questionable at the present moment. One way to proceed is to complement AFM measurements by instrumented indentation measurements at microscale and macroscale, in order to obtain better initial quantitative estimates of the volumetric and shear relaxation functions.

8. Discussion and recommendations

From simulations with the developed healing model, briefly described in the previous sections, it is evident that many different bitumen phase configurations can be formed from an initially homogeneous configuration. The initial configuration and the smallest local dispersions of the material can thereby have an important effect, as does the configurational and surface free energy potentials. The rate at which these changes occur is of great importance for the practical implications of this phenomenon relates to rest periods in the laboratory to assess the healing rates and the actual healing ability of the asphalt pavement. Mobility of the bitumen is thereby an important characteristic of the bitumen that affects the healing potential and should be determined. It can therefore be expected that enhancing the mobility of the bituminous phases will increase the healing rates and thus the pavement life time.

The configuration free energy potential of bitumen can be determined from the configuration free energy curves of the individual phases by assuming that in a certain composition only the phase with the lowest energy will exist. Equilibrium is then found when the chemical potential is homogeneous throughout the material. This does not, however, mean that the mass fraction has to be homogeneous. Inhomogeneous distribution of phase affects the ability for bitumen to transmit stresses through its matrix. Having knowledge about the bitumen configurational free energy potentials can therefore contribute to better predictions of the in-time evolution of its ability to transmit stresses and reduce damage propagation. Optimizing the bitumen phase diagrams to promote the

resilience for stress-endurance will therefore enhance the lifetime of the overall pavement. This means that molecular volumes, densities and solubility of the bitumen phases should be determined.

The surface free energy potential accounts for energy due to interfaces between the distinct phases. For diffuse interfaces this means that the free energy is dependent on both the local composition as well as its surroundings. In the developed healing model, the Cahn Hilliard approach is taken in which the generation and thicknesses of the interfaces depends on a gradient energy coefficient. Insight into the gradient energy coefficients of various bitumen would enable more accurate predictions into the evolution of damage and healing potential and would allow for an optimization of the long-term behaviour.

With the advent of more powerful experimental tools with better controlled environmental conditions, it is foreseen that future research will be able to accurately and more easily determine these parameter for bitumen. Research will continue to develop the predictive models and more insight into the fundamental parameters that influence the healing and damage resistance of bitumen will be generated. It can be envisioned that from this research, detailed databases with the most commonly used bitumen will be developed that can be included in future asphalt mixture and pavement design. Also, more detailed test procedures that would enable researchers and pavement engineers to measure these parameters for their own material will become available in the coming years.

9. References

Andersson, M. & Nilsson, F. (1995). A perturbation method used for static contact and low velocity impact. *International Journal of Impact Engineering*, Vol. 16, No. 5, pp.759-775, ISSN 0734-743X

Baker, H. (1742). *The Microscope Made Easy*, Science Heritage Ltd, ISBN 0940095033, Lincolnwood,IL. 1987 reprint

de Moraes, M.B., Pereira, R.B., Simao, R.A., Leite, L.F.M. (2010). High temperature AFM study of CAP 30/45 pen grade bitumen. *Journal of Microscopy*, Vol. 239, No. 1, pp. 46–53, ISSN 1365-2818

Giannnakopoulos, A. E. (2006). Elastic and Viscoelastic Indentation of Flat Surfaces by Pyramid Indentors. *Journal of Mechanics and Physics of Solids*, Vol. 54, No. 7, pp. 1305-1332, ISSN 0022-5096

Gouldstone, A., Chollacoop, N., Dao, M., Li, J., Minor, A. & Shen, Y.-L. (2007). Indentation Across Size Scales and Disciplines: Recent developments in experimentation and modeling. *Acta Materialia*, Vol. 55, No. 142, pp. 4015- 4039, ISSN 1359-6454

Graham, G. A. C. (1965). The contact problem in the linear theory of viscoelasticity. *International Journal of Engineering Sciences*, Vol. 3, No. 1, pp. 27-46, ISSN 0020-7225

Gunter, M. (2009). AFM Nanoindentation of Viscoelastic Materials with Large End-Radius Probes. *Journal of Polymer Science: Part B: Polymer Physics*, Vol. 47, No. 16, pp. 1573-1587, ISSN 0887-6266

Hesp, S.A.M., Iliuta, S. & Shirokoff, J.W. (2007). Reversible aging in asphalt binders. *Energy & fuels*, Vol. 21, No. 2, pp. 1112-1121, ISSN 0887-0624

Huang, G. & Lu, H. (2007). Measurements of Two independent Viscoelastic Functions by Nanoindentation. *Experimental Mechanics*, Vol. 47, No. 1, pp. 87-98, ISSN 0014-4851

Jäger, A., Lackner, R., Eisenmenger-Sittner, Ch. & Blab, R. (2004). Identification of four material phases in bitumen by atomic force microscopy. *Road Materials and Pavement Design*. Vol. 5, pp. 9–24, ISSN 1468-0629

Jäger A., Lackner, R. & Stangl, K. (2007). Microscale Characterization of Bitumen–Back-Analysis of Viscoelastic Properties by Means of Nanoindentation. *International Journal of Materials Research*, Vol. 98, No. 5, pp. 404-413, ISSN 1862-5282

Korsunsky, A.M. (2001). The Influence of Punch Blunting on the Elastic Indentation Response. Journal of Strain Analysis, Vol. 36, No. 4, pp. 391-400, ISSN 0309-3247

Kringos, N., Schmets, A., Pauli, T. & Scarpas, T. (2009a). A Finite Element Based Chemo-Mechanics Model to Simulate Healing of Bituminous Materials, *Proceedings of the international workshop on chemo-mechanics of bituminous materials*, pp. 69-75, ISBN 978-94-90284-04-6, Delf, The Netherlands, June 9-11, 2009

Kringos, N., Scarpas, A., Pauli, T. & Robertson, R. (2009b). A thermodynamic approach to healing in bitumen. In: *Advanced testing and characterization of bituminous materials*, Loizos, A., Partl, M.N. & Scarpas, T., pp. 123- 128, Taylor & Francis, ISBN 978-0-415-55854-9, London

Kringos, N., Pauli, T., Schmets, A. & Scarpas, T. (2012). Demonstration of a New Computational Model to Simulate Healing in Bitumen. *Journal of the Association of Asphalt Paving Technologists*, Under review

Larsson, P.-L. & Carlsson, S. (1998). On Microindentation of Viscoelastic Polymers. *Polymer Testing*, Vol. 17, No. 1, pp. 49-75, ISSN 0142-9418

Lee, E. H. & Radok, J. R. M. (1960). The contact problems for viscoelastic bodies. Journal of Applied Mechanics, Vol. 27, No. 3, pp. 438-444, ISSN 0021-8944

Lesueur, D., Gerard, J.-F., Claudy, P., Létoffé, J.-M., Planche, J.-P. & Martin, D. (1996). A structure-related model to describe asphalt linear viscoelasticity. *Journal of Rheology,* Vol. 40, No. 5, pp. 813–836, ISSN 0148-6055

Loeber, L., Sutton, O., Morel, J., Valleton, J.-M. & Muller, G. (1996). New direct observations of asphalts and asphalt binders by scanning electron microscopy and atomic force microscopy. *Journal of Microscopy*, Vol. 182, No. 1, pp. 32–39, ISSN 1365-2818

Loeber, L., Muller, G., Morel, J. & Sutton, O. (1998). Bitumen in colloidal science: a chemical, structural and rheological approach. *Fuel*, Vol. 77, No. 13, pp. 1443–1450, ISSN 0016-2361

Lu, X. & Redelius, P. (2006). Compositional and structural characterization of waxes isolated from bitumens. *Energy & fuels*, Vol. 20, No. 2, pp. 653-660, ISSN 0887-0624

Oliver, W. C. & Pharr, G. M. (1992). An Improved Technique For Determining Hardness and Elastic-Modulus Using Load and Displacement Sensing Indentation Experiments. *Journal of Materials Research*, Vol. 7, No. 6, pp. 1564-1583, ISSN 0884-2914

Oliver, W. C. & Pharr, G. M. (2003). Measurement of Hardness and Elastic Modulus by Instrumented Indentation: Advances in Understanding and Refinements to Methodology. *Journal of Materials Research*, Vol. 19, No. 1, pp. 3-20, ISSN 0884-2914

Pauli, A.T., Branthaver, J.F., Robertson, R.E., Grimes, W. and Eggleston, C.M. (2001). Atomic force microscopy investigation of SHRP asphalts. *ACS division of fuel chemistry preprints*, Vol. 46, No. 2, pp. 104-110

Pauli, A.T. & Grimes, W. (2003). Surface morphological stability modeling of SHRP asphalts. *ACS division of fuel chemistry preprints*, Vol. 48, No. 1, pp. 19-23

Pauli, A.T., Grimes, R.W., Beemer, A.G., Miller, J.J., Beiswenger, J.D. & Branthaver, J.F. (2009). Studies if the Physico-Chemical Nature of the SHRP Asphalts: PART-I & II, *Proceedings of the international workshop on chemo-mechanics of bituminous materials*, pp. 25-30 & 49-53, ISBN 978-94-90284-04-6, Delf, The Netherlands, June 9-11, 2009

Pauli, A.T., Grimes, R.W., Beemer, A.G., Turner, T.F. & Branthaver, J.F. (2011). Morphology of asphalts, asphalt fractions and model wax-doped asphalts studied by atomic force microscopy. *International Journal of Pavement Engineering*, Vol. 12, No. 4, pp. 291-309, ISSN 1029-8436

Redelius, P. (2009). Chemistry of Bitumen or Asphaltenes Where are you ? *Proceedings of the international workshop on chemo-mechanics of bituminous materials*, pp. 31-35, ISBN 978-94-90284-04-6, Delf, The Netherlands, June 9-11, 2009

Tarefder, R.A. & Arifuzzaman, M. (2010a). Nanoscale Evaluation of Moisture Damage in Polymer Modified Asphalts. *ASCE Journal of Materials in Civil Engineering*, Vol. 22, No. 7, pp. 714–725, ISSN 0899-1561

Tarefder, R.A., Zaman, A. & Uddin, W. (2010b). Determining Hardness and Elastic Modulus of Asphalt by Nanoindentation. *ASCE International Journal of Geomechanics*, Vol. 10, No. 3, pp. 106–116, ISSN 1532-3641

Tripathy, S. & Berger, E .J. (2009). Measuring Viscoelasticity of Soft Samples Using Atomic Force Microscopy. *Journal of Biomechanical Engineering-Transactions of the ASME*, Vol. 131, No. 9, pp. 094507, ISSN 0148-0731

Vanlandingham, M. R., Chang, N.-K., Drzal, P.L., White, C. C. & Chang, S.-H. (2005). Viscoelastic Characterization of Polymers Using Instrumented Indentation. I. Quasi-Static Testing. *Journal of Polymer Science: Part B: Polymer Physics*, Vol. 43, No. 14, pp.1794-1811, ISSN 0887-6266

Wu, S.P., Pang, L., Mo, L.-T., Chen, Y.-C. & Zhu, G.-J. (2009). Influence of aging on the evolution of structure, morphology and rheology of base and SBS modified bitumen. *Construction and Building Materials*, Vol. 23, No. 2, pp. 1005–1010, ISSN 0950-0618

Zhang, H., Wang, H. & Yu, J. (2011). Effect of aging on morphology of organo-montmorillonite modified bitumen by atomic force microscopy. *Journal of Microscopy*, Vol. 242, No. 1, pp. 37–45, ISSN 1365-2818

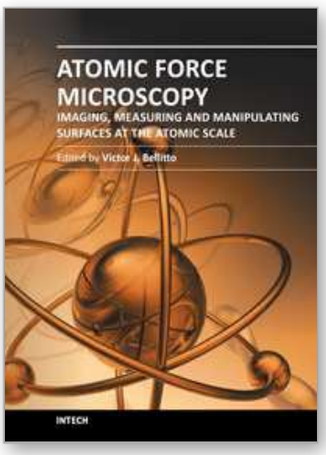

Atomic Force Microscopy - Imaging, Measuring and Manipulating Surfaces at the Atomic Scale

Edited by Dr. Victor Bellitto

ISBN 978-953-51-0414-8
Hard cover, 256 pages
Publisher InTech
Published online 23, March, 2012
Published in print edition March, 2012

With the advent of the atomic force microscope (AFM) came an extremely valuable analytical resource and technique useful for the qualitative and quantitative surface analysis with sub-nanometer resolution. In addition, samples studied with an AFM do not require any special pretreatments that may alter or damage the sample and permits a three dimensional investigation of the surface. This book presents a collection of current research from scientists throughout the world that employ atomic force microscopy in their investigations. The technique has become widely accepted and used in obtaining valuable data in a wide variety of fields. It is impressive to see how, in a short time period since its development in 1986, it has proliferated and found many uses throughout manufacturing, research and development.

InTech Europe
University Campus STeP Ri
Slavka Krautzeka 83/A
51000 Rijeka, Croatia
Phone: +385 (51) 770 447
Fax: +385 (51) 686 166
www.intechopen.com

InTech China
Unit 405, Office Block, Hotel Equatorial Shanghai
No.65, Yan An Road (West), Shanghai, 200040, China
中国上海市延安西路65号上海国际贵都大饭店办公楼405单元
Phone: +86-21-62489820
Fax: +86-21-62489821

IntechOpen